NASA Technical Memorandum 88819

High-Temperature Effect of Hydrogen on Sintered Alpha-Silicon Carbide

Gary W. Hallum and Thomas P. Herbell
Lewis Research Center
Cleveland, Ohio

Prepared for the
88th Annual Meeting of the American Ceramic Society
Chicago, Illinois, April 27—May 1, 1986

NASA

HIGH-TEMPERATURE EFFECT OF HYDROGEN ON SINTERED ALPHA-SILICON CARBIDE

by

Gary W. Hallum and Thomas P. Herbell
National Aeronautics and Space Administration
Lewis Research Center
Cleveland, Ohio 44135

ABSTRACT

Sintered alpha-silicon carbide was exposed to pure, dry hydrogen at high temperatures for up to 500 hr. Weight loss and corrosion were seen after 50 hr at temperatures as low as 1000 °C. Corrosion of SiC by hydrogen produced grain boundary deterioration at 1100 °C and a mixture of grain and grain boundary deterioration at 1300 °C. Statistically significant strength reductions were seen in samples exposed to hydrogen for times greater than 50 hr and temperatures above 1100 °C. Critical fracture origins were identified by fractography as either general grain boundary corrosion at 1100 °C or as corrosion pits at 1300 °C. A maximum strength decrease of approximately 33 percent was seen at 1100 and 1300 °C after a 500-hr exposure to hydrogen. A computer-assisted thermodynamic program was also used to predict possible reaction species of SiC and hydrogen.

E-3180

INTRODUCTION

Corrosion of silicon carbide (SiC) from exposure to hydrogen at high temperatures is a major concern for its use as a structural component in a ceramic Stirling engine. SiC offers several favorable characteristics over other structural ceramics and has therefore been selected for potential use for heat exchanger tubes. SiC has the high thermal conductivity needed for heat transfer to the working fluid (hydrogen gas). It also exhibits high strength at elevated temperatures and has a coefficient of thermal expansion

that is compatible with the proposed mullite pressure vessel. This latter fact may reduce any fabrication problems associated with joining SiC heater tubes to the mullite vessel.[1]

The operating temperature of the heater tubes is expected to approach 1300 °C. At this temperature, corrosion of SiC by hydrogen is possible. The corrosion may occur as uniform material loss and/or selective pitting resulting in a decrease in fracture strength.

The effect of high-temperature hydrogen on the microstructure of pressureless sintered alpha-silicon carbide (SASC) has been studied by Fischman and Brown.[2] Through thermodynamic calculations and experimental evaluation, they determined that the free carbon in the SiC is removed by hydrogen with a possible reaction with SiC also occurring. These thermodynamic and experimental studies were done with a 40:60 mixture of H_2:Ar at 1400 °C. Jero and Brown[3] evaluated the strength of SASC exposed to a 40:60 mixture of H_2:Ar at 1400 °C for 50 hr. Material loss was seen at the grain boundaries resulting in a 26-percent decrease in room-temperature fracture strength.

In the present investigation, the effect of pure, high-temperature hydrogen on the microstructure and retained room temperature strength of pressureless SASC was studied. The SASC was exposed to hydrogen for 50 hr at several temperatures between 1000 and 1400 °C. Hydrogen exposure times were also extended to 500 hr at 1100 and 1300 °C. Thermodynamic calculations were made to determine possible reaction species formed under various experimental conditions.

Single-crystal alpha-SiC was also exposed to high-temperature hydrogen. This was done to identify any corrosion effect on the surface of pure SiC.

PROCEDURE

The SASC* test bars used were 6 by 3 by 25 mm. The bars were cleaned ultrasonically in alcohol, measured, and weighed before each hydrogen test.

The single-crystal SiC was grown by vapor deposition in a graphite furnace. The basal plane was used for identifying possible surface reactions. The single-crystal SiC was cleaned in an HF solution to remove any surface oxide. The crystals were then exposed to hydrogen at 1100 and 1400 °C for 50 and 20 hr, respectively. Scanning electron microscopy (SEM) and x-ray energy dispersive spectroscopy (XEDS) were used to characterize the reacted surfaces.

The hydrogen was pure and dry with a water content of approximately 25 ppm. The flow rate of hydrogen over the samples was regulated at room temperature and kept at approximately 475 cc/min. A horizontal tube furnace equipped with a 99.8 percent pure Al_2O_3 tube was used. Test specimens were kept in a helium atmosphere until the test temperature was reached, then the atmosphere was switched to hydrogen. Cooldown was also done in helium.

Each run contained approximately 12 as-received test bars and a sample polished using a 3-μm diamond grit. The SiC samples were exposed to a range of temperatures for several different times as summarized in Table I. Upon completion of a run, the bars were removed from the furnace, weighed, and measured. Specimens were stressed to fracture using a four-point bending technique. Loading rate was 0.05 cm/min with an outer span of 1.90 cm and a inner span of 0.95 cm. Strengths were calculated using the following equation:

$$MOR = \frac{3P(L - a)}{2bd^2}$$

where P is the load at failure, L the outer span, a the inner span, b the specimen width, and d the specimen thickness. Original sample dimensions were used to calculate fracture stresses. However, results indicated that the surface recession due to any material loss was negligible (<40 μm) and had no significant effect (<4 percent) on the calculation of the strength.

* Sohio Engineered Materials, Niagara Falls, NY

The polished sample of sintered SiC and the corroded samples were characterized by several techniques. X-ray diffraction (XRD), SEM, and XEDS were used to examine and identify the mechanism of attack.

RESULTS

Morphology

The grain size of the SASC was determined to be approximately 6 μm with porosity between 1 to 2 percent. The as-received surface of the bars is shown in Fig. 1. Grinding marks on the surface can be seen resulting in a 15-μm rms finish with grinding pullouts up to 10 μm in diameter.

The SiC sample shown in Fig. 1 was characterized by x-ray photoelectron spectroscopy (XPS) indicating the presence of SiO_2 on the surface of the bars. In an attempt to remove the SiO_2 from the surface, the bars were polished to a 3-μm finish. This procedure only reduced the amount of surface SiO_2 but did not eliminate it. Polishing, however, did help identify free carbon in the SASC material. The carbon, identified by windowless XEDS, existed in concentrated pockets throughout the material as shown in Fig. 2.

The surface of the SiC single crystal is shown in Fig. 3. The crystal was treated with a light HF etchant to remove any possible oxide. Optical microscopy showed no change in the surface after this treatment.

Attack Morphology

Figure 4 shows the effect of temperature on the surface of the as-received material after exposure to hydrogen for 50 hr. The surface remained relatively unchanged, as compared to Fig. 1, at 1000 °C (Fig. 4(a)) with only a slight amount of grain boundary corrosion. The amount of grain boundary corrosion increased at 1100 °C (Fig. 4(b)). At exposure times longer than 50 hr at 1100 °C, corrosion between grains became so extreme that the individual grains

were loose on the surface. Loosening of the grains occurred after only 50 hr at 1200 °C (Fig. 4(c)) indicating the strong influence of temperature. At 1300 °C, severe grain boundary deterioration occurred along with the attack of individual SiC grains. The SiC grains were also loose and easily removed. Similar results were seen at 1400 °C (Fig. 4(d)) after a 50 hr exposure. Several observations indicated that the SiC grains were preferentially attacked along certain crystallographic directions at 1300 °C and above. The attack appeared to occur parallel to the basal plane of the SiC.

The corrosion layer on the surface of the bars reached a thickness of approximately 30 μm after exposure at 1300 °C for 500 hr. Voids on the surface of the bar were further enhanced by removing grain boundary material and thus extending the voids deeper into the specimen.

Polished samples of sintered SiC showed similar signs of hydrogen corrosion as the 15-μm ground test bars. Grain and grain boundary corrosion were present in all samples treated above 1300 °C. Below 1300 °C, corrosion was prevalent in the grain boundaries. Whiskers of submicrometer size formed on the surface of the sample below 1300 °C. The whiskers were random in orientation and were found in greater concentrations inside voids. These whiskers, shown in Fig. 5, were found to contain silicon and oxygen indicating SiO_2. Further characterization using selected area diffraction (SAD) on the TEM indicated that the whiskers were also amorphous.

The formation of whiskers was also seen to occur on the surface of the single-crystal SiC below 1300 °C in hydrogen. These whiskers were identical to those that formed on the surface of the polished SiC. Above 1300 °C, no whiskers were formed; however, the hydrogen preferentially attacked regions of the crystal leaving hexagonal shaped pits on the surface. These pits, shown in Fig. 6, were assumed to be dislocations in the crystal lattice etched by hydrogen.[4]

Weight Loss and Strength

The rate of weight loss of SASC in the first 50 hr of exposure to hydrogen is shown in Fig. 7. The weight loss remained small between 1000 and 1300 °C after 50 hr. At 1300 °C, the rate of weight loss increased significantly. As seen previously in Fig. 4, the majority of weight loss in the first 50 hr occurred at the grain boundaries exposing the SiC grains on the surface. Weight loss further increased at 1100 and 1300 °C for times greater than 50 hr showing possible linear weight loss as a function of time. The majority of material loss again occurred at the grain boundaries with additional corrosion of the SiC grains occurring at 1300 °C.

Material loss of the individual bars was also dependent on their distance from neighboring bars with the amount of loss decreasing as the distance between bars decreased. Test bars isolated from other bars showed even greater weight loss.

The fracture strength of the as-received SASC bars was determined to be 506 MPa, which was somewhat higher than previously published strengths of 335 to 425 MPa.[5-8] The higher strength can be attributed to the smaller and more equiaxed grains found in this SASC. Large standard deviations for all strengths made it necessary to use the student t-distribution at a 95-percent confidence interval to make any statistical comparisons with the baseline fracture strength. Table II contains strength data from all fracture tests and statistical comparisons in this study.

The effect of temperature on the room-temperature fracture strength of SASC after a 50-hr exposure to hydrogen is shown in Fig. 8. Statistical analysis indicated significant reductions in room-temperature strength from the baseline strength in SASC bars exposed to hydrogen for 50 hr at 1000 °C

and above 1200 °C. It is unclear why there was no strength reduction seen at 1100 °C. The maximum decrease in strength was seen after exposure to hydrogen at 1400 °C.

Fracture strength degradation as a function of exposure time at 1100 and 1300 °C is shown in Fig. 9. Fracture strength decreased linearly with time for bars exposed to hydrogen at 1100 °C. This steady decrease in strength can be attributed to the increasing material loss at grain boundaries. At 1300 °C, a rapid decrease in fracture strength occurred in the first 50 hr of hydrogen exposure. This decrease in strength occurs with the formation of corrosion pits on the surface of the bars. These pits, possibly areas of high carbon concentration, were enhanced with time, further decreasing the fracture strength. Although the rate of strength degradation at 1100 and 1300 °C was different, a strength decrease of approximately 33 percent was seen after 500 hr of hydrogen exposure at either temperature. Thus, after extended exposure to hydrogen at 1100 and 1300 °C, the different modes of corrosion had similar effects on the fracture strength.

Fractography

Fracture origins were identified by SEM and optical microscopy. The location of critical flaws was determined by following radial crack lines to the fracture origin. The fracture surfaces indicated a mixture of both intergranular and transgranular fracture.

The baseline SASC material, unexposed to hydrogen, exhibited mostly subsurface flaws. These flaws were identified as either pores or agglomerates that had high aspect ratios and were typically 20 to 50 μm below the tensile surface. Examples of these internal flaws are shown in Fig. 10. Similar subsurface fracture origins were also predominant in SASC exposed to hydrogen at 1000 and 1100 °C for 50 hr. As corrosion and subsequent weight loss progressed, critical fracture origins were increasingly found on the tensile

surface. This transition from subsurface flaws to tensile surface flaws occurred between 1100 and 1300 °C indicating the first effects of corrosion. As exposure times increased past 100 hr at 1100 °C, the corrosion occurred mostly in the grain boundaries of the material lowering the fracture strength with increased exposure. After 500 hr of exposure to hydrogen at 1100 °C, fracture origins were found to be large areas of surface corrosion and not corrosion pits as seen in Fig. 11.

Above 1200 °C, the material loss at the grain boundaries occurred along with selective pitting. These pits eventually replace subsurface flaws as critical fracture origins. The depth of the critical flaws on the surface ranged from 20 to 200 μm depending on the amount of corrosion. Pre-existing flaws on the surface were further enhanced by hydrogen corrosion. An example of a typical surface flaw, found on a sample exposed to hydrogen for 500 hr at 1300 °C, is shown in Fig. 12. As the temperature and time of exposure to hydrogen increased, grain boundary corrosion in the voids became more severe and deeper. Enhancement of voids was seen to occur at times of only 50 hr at 1300 °C. The fact that surface voids were enhanced above 1300 °C may explain the sharper rate of strength decrease in the first 50 hr of exposure at 1300 °C in Fig. 9 as compared to SASC bars exposed to hydrogen at 1100 °C where grain boundary corrosion was prevalent.

DISCUSSION

A theoretical study was done to determine the thermodynamics of hydrogenation of SiC. A computer program[9] was used to calculate the presence of possible reaction products, at equilibrium, given the thermodynamic data for the initial reactants.[10] In this case, the initial reactants were Si, C, H, and O. Several species containing these elements were considered. The computer program calculated the equilibrium compositions, using the thermodynamic data for these species, by minimizing Gibbs free energy. The calculation assumed

that all the gases formed were ideal and formed ideal mixtures and that the condensed phases were pure. The program calculated the mole fractions of possible species at equilibrium that exceeded 10E-12 mole fraction at a pressure of 1 atm between 700 and 1700 °C. The mole fractions were then plotted against temperature. Although the method used to calculate the mole fraction of any reaction species was only theoretical, it was important because it considered the actual hydrogenation process. Several assumptions were made to obtain this plot. The SiC was assumed not to have a surface scale of SiO_2 or free carbon, a limited amount of reactant species was present, and complete equilibrium had been reached.

In this theoretical system, 100 moles of hydrogen and 10 moles of SiC were the initial reactants that were allowed to reach equilibrium. The calculated product species are shown in Fig. 13. The predominant carbon-based molecule formed was methane with its equilibrium concentration remaining constant at all temperatures. Additional hydrocarbons were formed as the temperature of the system increased. Decarburization left a silicon-rich surface behind that remained stable up to the melting point of silicon at 1410 °C. Hydrogen reactions with silicon formed predominantly silane, the most stable of the silicon-hydrogen molecules. These results are in agreement with Fischmans[2] thermodynamic computer calculations.

The same program was used with an environment containing 25 ppm of water in the hydrogen. The amounts of product species are shown in Fig. 14. The presence of water vapor in the system slightly reduced the equilibrium amount of methane and silane at all temperatures. However, the presence of the water contributed to passive oxidation of the SiC below 1100 °C forming SiO_2. Above 1100 °C, SiO_2 was removed and active oxidation occurred forming SiO and CO. Above 900 °C, SiO eventually became the predominant silicon-based molecule

at equilibrium. These data indicated that the presence of water vapor in the system resulted in thermodynamically favorable oxidation reactions.

It is important to consider that this computer program was used only as a guide to predict possible reaction species. The systems were closed and allowed to reach equilibrium with only the initial reactants present. Furthermore, the kinetics of the individual reactions were not considered. However, these calculated results do provide possible reaction paths.

A direct microstructural observation was used to evaluate the actual hydrogenation process involving two steps: (1) reduction and removal of SiO_2 and free carbon from the surface and (2) reaction of hydrogen with SiC. It has already been seen that SASC exposure to hydrogen led to general material loss and fracture strength degradation. This agrees with thermodynamic calculations where free carbon reacted with hydrogen or oxygen to form methane (CH_4) and carbon monoxide (CO), respectively. Furthermore, XPS studies revealed that the SiO_2 layer and free carbon on the surface are removed before any SiC grain degradation.

The removal of carbon can occur by several processes. The two considered in this study are shown by reactions (1) and (2):

$$C + 2H_2 \longrightarrow CH_4 \qquad (1)$$

$$C + H_2O \longrightarrow CO + H_2 \qquad (2)$$

Carbon may react to form methane or reduce the water present in the system to form CO and additional hydrogen. The formation of CO is thermodynamically favored over the formation of CH_4; however, the large amount of hydrogen already present suppresses reaction (2) and contributes more to reaction (1).

The reduction of the SiO_2 layer on the surface of the SASC bars by hydrogen occurs most likely by reaction (3):

$$SiO_2 + H_2 \longrightarrow SiO + H_2O \qquad (3)$$

This produces gaseous SiO that is unstable at lower temperatures and may condense out as SiO_2.

The precise mechanism of SiC corrosion remains uncertain. Although corrosion of the individual grains does take place, as seen in Fig. 5, only general theories of the mechanisms of corrosion can be provided at this time.

SiC may react with hydrogen or water in several possible ways. Reactions (4) to (6) were identified by using thermodynamics as a guide:

$$SiC + 2H_2 \longrightarrow Si + CH_4 \quad (4)$$

$$SiC + 4H_2 \longrightarrow SiH_4 + CH_4 \quad (5)$$

$$SiC + 2H_2O \longrightarrow SiO + CO + 2H_2 \quad (6)$$

Reactions (4) and (5) are thermodynamically unfavorable, but some SiH_4 will form because reaction products are constantly being removed from the system by the flowing hydrogen. The species SiH_4 is very unstable and conditions at the end of the furnace may favor its decomposition into silicon. This decomposition reaction would explain the silicon fibers found at the end of the furnace after exposure tests above 1300 °C where weight loss is the largest. Regardless of which of the previous reactions ((4) to (6)) predominates, the amount of product species appears to increase with temperature resulting in a higher rate of weight loss for SASC as seen in Fig. 7.

The presence of water in the system contributes SiO and CO to the system resulting in active oxidation.[6] Because of the much lower free energy of reaction (6) compared to reactions (4) and (5), it is possible for SiO or CO to become the predominant product species with higher concentration levels of water. This fact emphasizes the importance of the concentration of water affecting the final corrosion process.

The possibility that active oxidation of the silicon occurs after the removal of carbon may also explain the formation of SiO_2 whiskers on the

surface of polished SASC samples. Similar whisker formation was seen by Hinze and Graham[11] during the active oxidation of silicon. The formation of these whiskers is believed to occur by vaporization-condensation processes. Local variations in oxygen partial pressure may allow the formation of SiO in crevices and subsequent passive oxidation to SiO_2 whiskers.

The general kinetics of gas-solid reactions were studied by Chilton.[12] Chilton presented possible steps in a general reaction process. The reduction reaction can be controlled by (1) gaseous diffusion through a boundary layer, (2) surface reaction, (3) the transition between them, and (4) the transfer of product species from the outer surface to the bulk gas. Any one of these processes may control the overall rate of reaction. The reduction and concurrent weight loss of SASC was found to depend on the orientation and distance between bars in the furnace. This position dependence supports reactions (1) to (6) and indicates that gas phase transport through the boundary layer may be rate limiting. Dependence on the flow rate of the surrounding gas also suggests gas phase transport may be rate limiting.

SUMMARY

Pressureless sintered alpha-SiC was exposed to high-temperature hydrogen for up to 500 hr. Weight loss and general surface corrosion were seen after 50 hr at temperatures as low as 1000 °C. Surface corrosion was in the form of grain boundary deterioration in samples tested at 1100 °C. Grain and grain boundary corrosion became prevalent as the exposure temperature approached 1300 °C. Statistically significant strength reductions were seen in samples exposed to hydrogen for times greater than 50 hr above 1100 °C. Fracture origins were found on the tensile surface where corrosion had been extreme. Fractography revealed that fracture origins of samples exposed to hydrogen at 1100 °C were areas of grain boundary deterioration. Fracture origins of samples exposed at 1300 °C for 50 hr or more were found to have corrosion pits

on the tensile surface and general grain boundary deterioration. Although the attack morphology of samples exposed to hydrogen at 1100 and 1300 °C were different, the final strength after 500 hr at both these temperatures was found to decrease approximately 33 percent.

CONCLUSIONS

The room temperature fracture strength of SASC is severely degraded by a hydrogen plus 25 ppm water environment at the operating temperature of the proposed ceramic Stirling engine. Thermodynamic calculations indicate that there is a potential for doping the hydrogen to inhibit the corrosion of SASC. Methane, a product of the reduction reaction, is a possible dopant. However, further experimental work is needed to evaluate the effect of dopants on the microstructure and fracture strength of SASC.

REFERENCES

1. S. Musikant, W. Chiu, D. Darooka, and D. Mullings, "Ceramic Automotive Stirling Engine Study," NASA CR-174907, 1985. (DOE/NASA/0312-1)

2. G. Fischman, S.D. Brown, and A. Zangvil, "Hydrogenation of SiC: Theory and Experiments," Mater. Sci. Eng., 71, 295-302 (1985).

3. P.D.Jero and S. Brown, "The Effect of High Temperature Hydrogenation on the Fracture Strength of a Sintered Alpha SiC," presented at the 87th Annual American Ceramic Society Meeting, Chicago, Il, May 8, 1985.

4. S. Amelinckx and G. Strumane, "Surface Features on Silicon Carbide Crystal Faces," pp. 162-199 in Silicon Carbide, edited by J.R. O'Conner and J. Smiltens, Pergamon Press, New York, 1960.

5. R.K. Goliva, "Phenomenology of Fracture in Sintered Alpha Silicon Carbide," J. Mater. Sci., 19, 2111-2120 (1984).

6. P.F. Becher, "Strength Retention in SiC Ceramics After Long-Term Oxidation," J.Am. Ceram. Soc., 66, C-120 - C-121 (1983).

7. J.L. Smialek and N.S. Jacobson, "Mechanism of Strength Degradation for Hot Corrosion of Alpha-SiC," NASA TM-87052, 1984.

8. R.C. Bradt, "The Impact Resistance of SiC and Other Mechanical Properties of SiC and Si_3N_4, NASA CR-165325, 1984.

9. S. Gordon and B.J. McBride, "Computer Program for Calculation of Complex Chemical Equilibrium Compositions, Rocket Performance, Incident and Reflected Shocks, and Chapman-Jouquet Detonations," NASA SP-273, 1976.

10. D.R. Stull and H. Prophet, eds., JANAF Thermochemical Tables, 2nd ed., National Bureau of Standards, 1971.

11. J.W. Hinze and H.C. Graham, "The Active Oxidation of Silicon and Silicon Carbide in the Viscous Gas-Flow Regime," J. Electrochem. Soc., 123, 1066-1073, (1976).

12. T.H. Chilton and A.P. Colburn, "Mass Transfer (Absorption) Coefficients," Ind. Eng. Chem., 26, 1183-1187 (1934).

TABLE I. - TEMPERATURE AND HYDROGEN EXPOSURE TIMES FOR SINTERED ALPHA-SILICON CARBIDE

Time, hr	Temperature, °C					
	1000	1100	1200	1300	1350	1400
	Total number of bars tested					
50	13	20	12	12	13	11
100	--	27	--	12	--	--
500	00	9	--	9	--	--

TABLE II. - EFFECT OF HIGH-TEMPERATURE HYDROGEN EXPOSURE ON ROOM-TEMPERATURE FRACTURE STRENGTH

Exposure temperature, °C	Exposure time, hr	Sample size, h	Average strength, MPa, $\bar{\sigma}_p$	Standard deviation, MPa, S_i	95 Percent confidence interval of MPa, $\bar{\sigma}_f$	Significant strength reduction from room temperature
As-received	---	12	506	65	463, 549	---
1000	50	13	428	55	395, 461	Yes
1100	↓	12	496	67	453, 538	No
1200	↓	12	429	103	363, 494	Yes
1300	↓	12	380	44	352, 408	↓
1350	↓	13	422	73	372, 466	↓
1400	↓	11	386	52	351, 420	↓
1100	100	13	473	78	423, 524	↓
1300	100	13	399	76	352, 445	↓
1100	500	9	342	53	292, 381	↓
1300	500	8	334	54	293, 376	↓

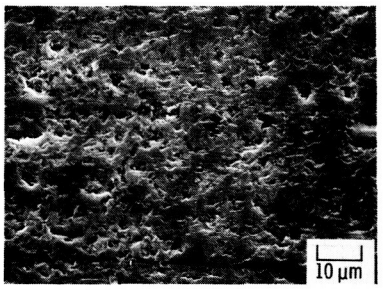

FIGURE 1.- SURFACE OF AS-RECEIVED SINTERED ALPHA-SILICON CARBIDE BARS REVEALING GRINDING MARKS AND SURFACE DAMAGE.

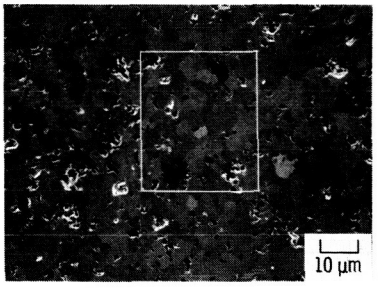

FIGURE 2.- LOCALIZED REGIONS OF CARBON SEEN A POLISHED SAMPLE OF SINTERED ALPHA-SILICON CARBIDE.

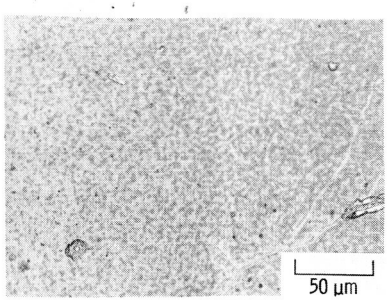

FIGURE 3.- SURFACE OF SINGLE-CRYSTAL ALPHA-SILICON CARBIDE ETCHED WITH A 8: 1 H_2O: HF SOLUTION.

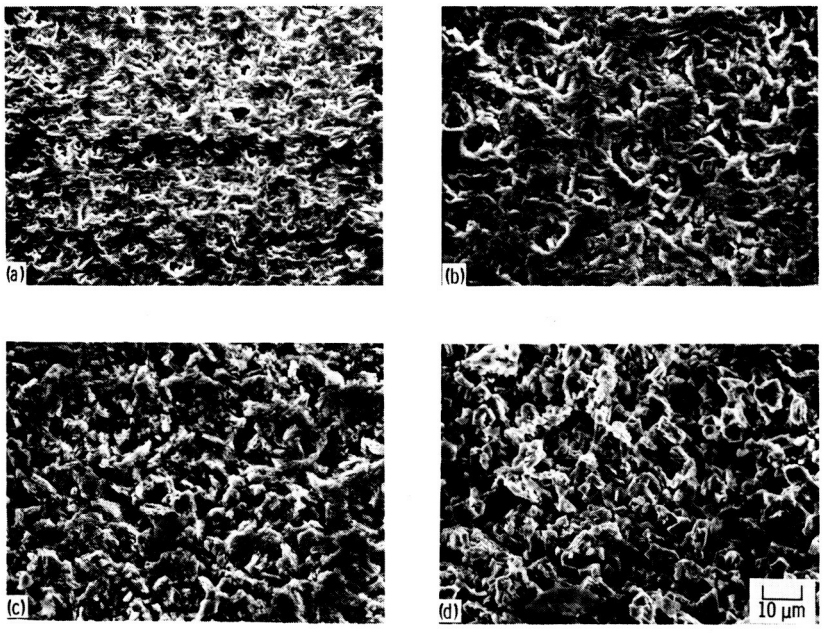

FIGURE 4.- CORROSION ON SURFACE OF SINTERED ALPHA-SILICON CARBIDE AFTER EXPOSURE TO HYDROGEN FOR 50 HOURS AT: (A) 1000 °C; (B) 1100 °C; (C) 1200 °C; AND (D) 1400 °C.

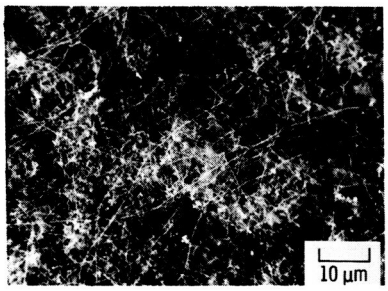

FIGURE 5.- FORMATION OF WHISKERS ON POLISHED SURFACE OF SINTERED ALPHA-SILICON CARBIDE EXPOSED TO HYDROGEN AT 1011 °C FOR 50 HR.

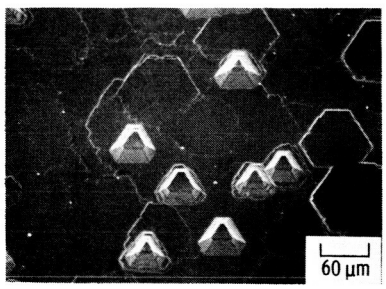

FIGURE 6.- DISLOCATION ETCH PITS ON SURFACE OF SINGLE-CRYSTAL ALPHA-SILICON CARBIDE EXPOSURE TO HYDROGEN AT 1400 °C FOR 50 HR.

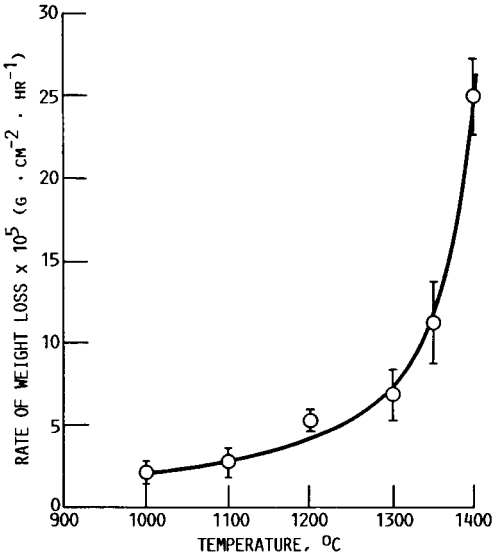

FIGURE 7. - EFFECT OF EXPOSURE TEMPERATURE ON THE RATE OF WEIGHT LOSS FOR SINTERED ALPHA-SILICON CARBIDE BARS EXPOSED TO HYDROGEN.

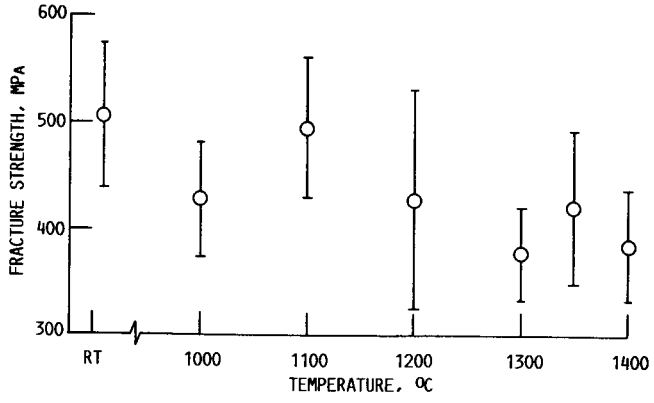

FIGURE 8. - EFFECT OF EXPOSURE TEMPERATUARE ON THE ROOM TEMPERATURE FRACTURE STRENGTH OF SINTERED ALPHA-SILICON CARBIDE BARS EXPOSED TO HYDROGEN FOR 50 HR. (RT = BASELINE ROOM TEMPERATURE STRENGTH.)

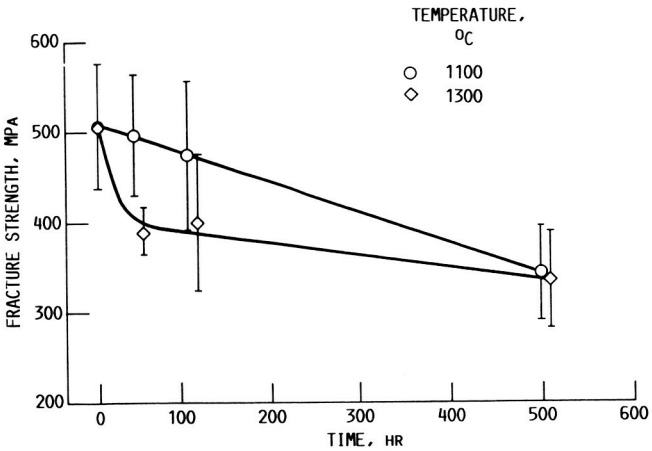

FIGURE 9. - EFFECT OF EXPOSURE TIME ON THE ROOM TEMPERATURE FRACTURE STRENGTH OF SINTERED ALPHA-SILICON CARBIDE AFTER EXPOSURE TO HYDROGEN AT 1100 AND 1300 °C. BASELINE STRENGTH INDICATED AT 0 HR.

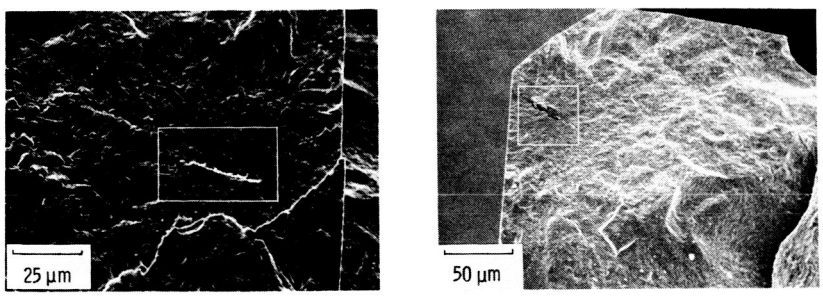

FIGURE 10. - TYPICAL SUBSURFACE FLAWS FOUND IN SINTERED ALPHA-SILICON CARBIDE IN MATERIAL UNEXPOSED TO HYDROGEN.

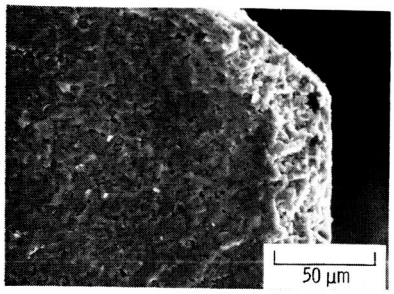

FIGURE 11. - SURFACE CORROSION ON SINTER ALPHA-SLICON CARBIDE EXPOSED TO HYDROGEN AT 100 ^{0}C FOR 500 HRS.

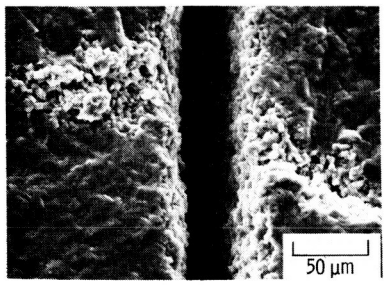

FIGURE 12. - CRITICAL FRACTURE ORIGIN IDENTIFIED AS CORROSION PIT. SAMPLE EXPOSED TO HYDROGEN AT 1300 ^{0}C FOR 500 HRS.

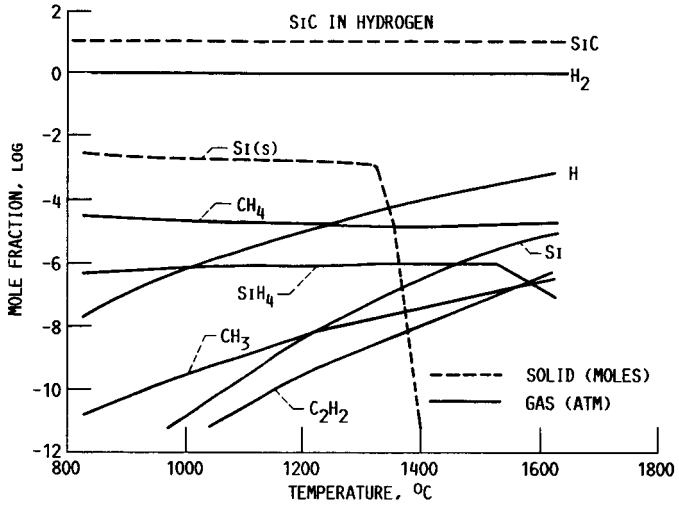

FIGURE 13. - CALCULATED REACTION PRODUCTS IN A SYSTEM CONTAINING 10 MOLES OF SILICON CARBIDE AND 100 MOLES OF HYDROGEN.

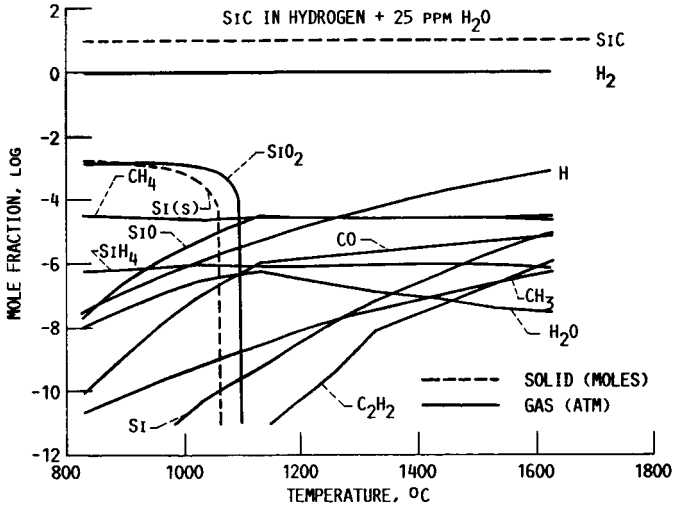

FIGURE 14. - CALCULATED REACTION PRODUCTS IN A SYSTEM CONTAINING 10 MOLES SILICON CARBIDE AND 100 MOLES HYDROGEN WITH 25 PPM WATER.

1. Report No.	2. Government Accession No.	3. Recipient's Catalog No.
NASA TM 88819		

4. Title and Subtitle	5. Report Date
High-Temperature Effect of Hydrogen on Sintered Alpha-Silicon Carbide	6. Performing Organization Code: 778-35-13

7. Author(s)	8. Performing Organization Report No.
Gary W. Hallum and Thomas P. Herbell	E-3180
	10. Work Unit No.

9. Performing Organization Name and Address	11. Contract or Grant No.
National Aeronautics and Space Administration Lewis Research Center Cleveland, Ohio 44135	13. Type of Report and Period Covered: Technical Memorandum

12. Sponsoring Agency Name and Address	14. Sponsoring Agency Code
National Aeronautics and Space Administration Washington, D.C. 20546	

15. Supplementary Notes

Prepared for the 88th Annual Meeting of the American Ceramic Society, Chicago, Illinois, April 27 - May 1, 1986.

16. Abstract

Sintered alpha-silicon carbide was exposed to pure, dry hydrogen at high temperatures for times up to 500 hr. Weight loss and corrosion were seen after 50 hr at temperatures as low as 1000 °C. Corrosion of SiC by hydrogen produced grain boundary deterioration at 1100 °C and a mixture of grain and grain boundary deterioration at 1300 °C. Statistically significant strength reductions were seen in samples exposed to hydrogen for times greater than 50 hr and temperatures above 1100 °C. Critical fracture origins were identified by fractography as either general grain boundary corrosion at 1100 °C or as corrosion pits at 1300 °C. A maximum strength decrease of approximately 33 percent was seen at 1100 and 1300 °C after 500 hr exposure to hydrogen. A computer assisted thermodynamic program was also used to predict possible reaction species of SiC and hydrogen.

17. Key Words (Suggested by Author(s))	18. Distribution Statement
Alpha-SiC; Hydrogen; Corrosion; Strength	Unclassified - unlimited STAR Category 27

19. Security Classif. (of this report)	20. Security Classif. (of this page)	21. No. of pages	22. Price*
Unclassified	Unclassified		

*For sale by the National Technical Information Service, Springfield, Virginia 22161